The Developmental Pattern of the Musculature Associated with the Mandibular and Hyoid Arches in the Longnose Gar, *Lepisosteus osseus* (Actinopterygii, Ginglymodi, Lepisosteiformes)

Peter Konstantinidis[1], Peter Warth[2], Benjamin Naumann[2], Brian Metscher[3], Eric J. Hilton[1], and Lennart Olsson[2]

This is the first in a planned series of studies in which we examine the cranial muscle ontogeny of exemplar taxa of actinopterygian clades to obtain a better understanding of the evolution of the cranial musculoskeletal system within the Actinopterygii. The Longnose Gar, *Lepisosteus osseus*, is a member of the basal actinopterygian family Lepisosteidae. Juvenile and adult gars are highly derived and anatomical characters can easily be misinterpreted, which makes a comparison with other taxa difficult. Highly complex adult structures such as the cranial skeleton and musculature are organized more simply early in development, making comparisons and homology assessments easier. Established methods such as clearing and double staining are widely used to study skeletal structures. However, methods to analyze the ontogeny of soft tissues are scarce. To study the development of the cranial musculature of *L. osseus*, we used a combination of 3D-reconstruction of soft tissue μCT scans and whole-mount antibody staining. The elongation of the palatoquadrate and the dentary that form the long snout of gars begins late in ontogeny. However, the adductor mandibulae complex, which separates from the mandibular muscle primordium initially as a single portion, does not follow the extension of the palatoquadrate. We also show that the ceratomandibular ligament that attaches the ceratohyal with the retroarticular process of the lower jaw is homologous with the mandibulohyoid ligament.

EXTANT gars of the family Lepisosteidae are classified in two genera, with four species in the genus *Lepisosteus* (*L. osseus, L. platostomus, L. oculatus, L. platyrhinchus*) and three in the genus *Atractosteus* (*A. tropicus, A. spatula, A. tristoechus*). The gars of the genus *Lepisosteus* are known from central North America, whereas the gars of the genus *Atractosteus* are known from southeastern North America, Central America, and Cuba. All species are restricted to freshwater, but *Atractosteus spatula, A. tristoechus* (Cavin, 2010; Grande, 2010), and *L. osseus* occasionally occur also in brackish and saltwater environments (Jenkins and Burkhead, 1993). The lepisosteids are the remnants of the Ginglymodi, a morphologically diverse actinopterygian division that includes three orders, the Lepisosteiformes, †Semionotiformes, and †Macrosemiiformes. Members of the Ginglymodi first appeared in the fossil record in deposits of the Early Cretaceous (†*Obaichthys*, †*Dentilepisosteus*), showing their maximum diversity in the Late Cretaceous (Wiley, 1976; Grande, 2010).

Together with the halecomorph and teleostean fishes, the Ginglymodi form the Neopterygii. The relationships among the three major divisions within Neopterygii were broadly debated until recently. The Ginglymodi were either considered to be the sister of the Halecostomi, a clade formed by the halecomorph and teleostean fishes (Gardiner, 1960; Patterson, 1973; Wiley, 1976; Rosen et al., 1981; Lauder and Liem, 1983; Gardiner et al., 1996) or the sister group of Halecomorphi to form the Holostei, which was considered to be the sistergroup of Teleostei (Huxley, 1861; Goodrich, 1930; Romer, 1966; Jarvik, 1980; Grande, 2010). Molecular phylogenetic studies have generally supported the Holostei hypothesis (Normark et al., 1991; Olsen and McCune, 1991; Lecointre et al., 1994, Inoue et al., 2003; Betancur-R. et al., 2013). However, it was not until Grande (2010) defined a new family of lepisosteiforms from the Cretaceous (†Obaichthyidae) that Holostei was morphologically diagnosed based on synapomorphies and displaced the hypothesis of Halecostomi as a monophyletic group.

Due to their basal phylogenetic position, gars have been of special interest to scientists since the nineteenth century. Certain aspects of gar morphology were either included in more comprehensive studies to uncover major evolutionary trends in vertebrate evolution (Gegenbaur, 1887; Sewertzoff, 1895; Luther, 1913; Schmalhausen, 1913; Kryzanovsky, 1927; Edgeworth, 1935; Jessen, 1972; Lauder, 1980a, 1980b; Arratia and Schultze, 1991; Britz and Johnson, 2010) or were the sole taxonomic focus of study; Veit (1907), Mayhew, (1924) and Hammarberg (1937) investigated the skull, Long and Ballard (2001) described the external development of the Longnose Gar, and Kammerer et al. (2006) and Hilton et al. (2014) described certain aspects of the jaws. The most extensive treatises on Lepisosteiformes are those of Wiley (1976) and Grande (2010), covering aspects of anatomy, phylogeny, and biogeography of both fossil and extant representatives. Despite the extensive literature on gars, studies of soft tissue, such as muscles and nerves, are rare (Gegenbaur, 1887; Luther, 1913; Lauder, 1980a), and Edgeworth's (1911, 1929, 1935) work on the cranial musculature of vertebrates are the only studies of soft tissues of gars to include an ontogenetic perspective.

Ontogenetic information has often provided a rich source to uncover aspects of homology of complex anatomical characters important for comparative morphology and systematics of fishes (Hilton et al., 2015, in this volume), especially in cases where species undergo drastic transformational changes (Fig. 1). One reason for the lack of ontogenetic studies of soft tissue was that it is not as accessible as the skeleton, due to the lack of standard methods (such as clearing and staining) that complements the very detailed but cost- and labor-intensive histology.

[1] Virginia Institute of Marine Science, College of William and Mary, Gloucester Point, Virginia 23062; E-mail: (PK) peterk@vims.edu. Send reprint requests to PK.
[2] Friedrich Schiller University, Institute of Systematic Zoology and Evolutionary Biology with Phyletic Museum, 07743 Jena, Germany.
[3] University of Vienna, Department of Theoretical Biology, 1090 Vienna, Austria.
Submitted: 12 November 2014. Accepted: 26 March 2015. Associate Editor: G. Arratia.
 DOI: 10.1643/OT-14-195 Published online: November 19, 2015

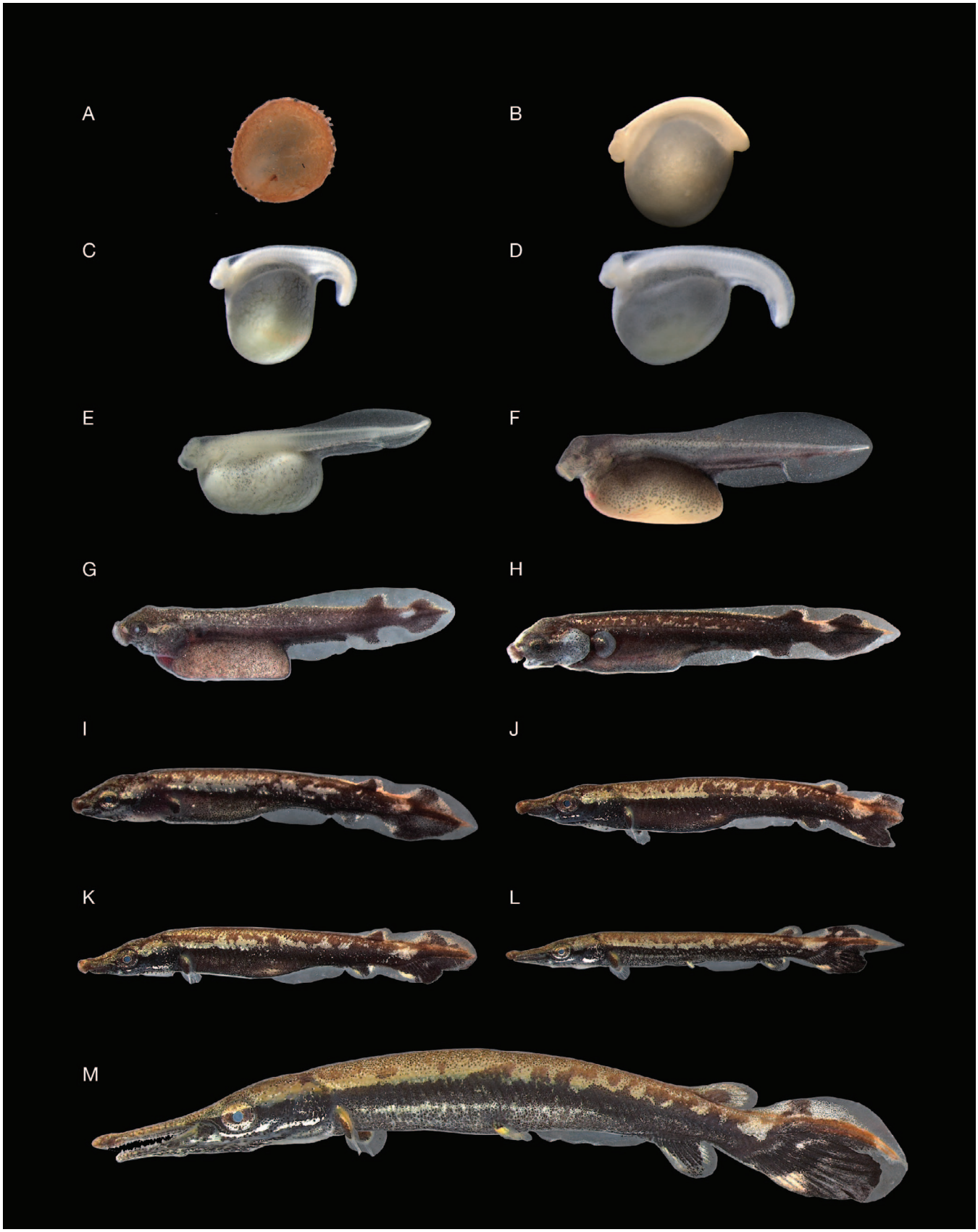

Fig. 1. Ontogenetic series of *Lepisosteus osseus*. The specimens are arranged in a developmental order rather than according to their actual size. The diameter of the (A) egg is 4.5 mm and lengths of other specimens are as follows: (B) 2.6 mm NL; (C) 4.8 mm NL; (D) 5.6 mm NL; (E) 7.8 mm NL; (F) 9.0 mm NL; (G) 13.2 mm NL; (H) 16.9 mm NL; (I) 16.3 mm SL; (J) 16.7 mm SL; (K) 18.6 mm SL; (L) 23.0 mm SL; (M) 34.0 mm SL.

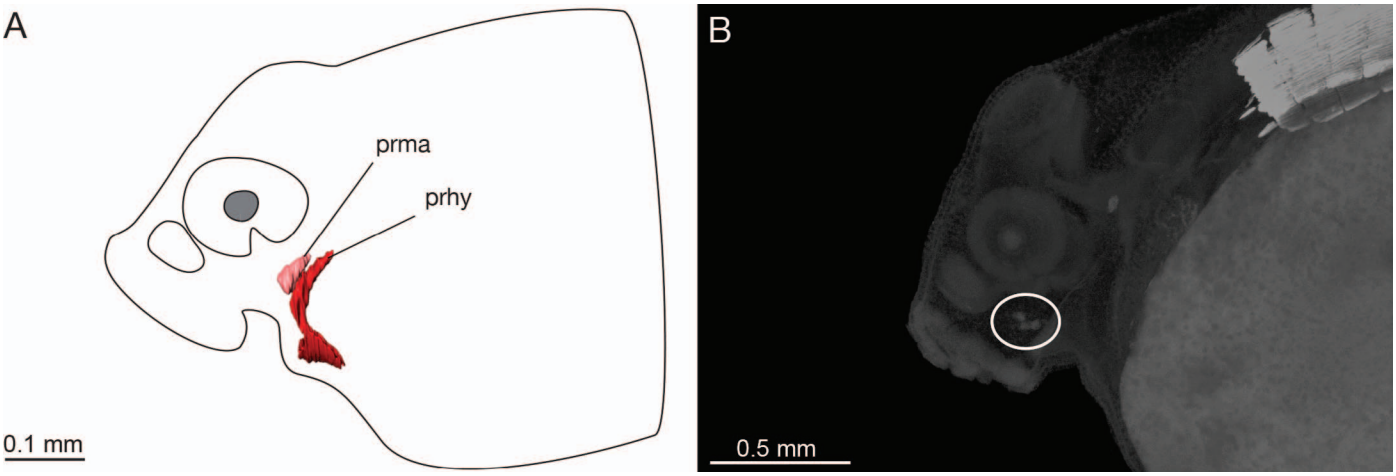

Fig. 2. (A) Lateral view of a reconstruction of a μCT scan of a 6.2 mm NL *Lepisosteus osseus*. (B) Lateral view of a confocal image of a 7.2 mm NL Longnose Gar. Abbreviations: prhy, hyomandibularis primordium; prma, mandibularis primordium.

However, methods originally used in developmental biology to study soft tissue have recently been used in comparative morphological studies (e.g., immunohistochemical methods; Hernandez et al., 2002; Ericsson and Olsson, 2004; Piekarski and Olsson, 2007; Staab and Hernandez, 2010; Uji et al., 2010, 2013; Konstantinidis and Harris, 2011), and new methods, such as μCT scanning, are becoming available (Metscher, 2009a; Werneburg and Hertwig, 2009). In this paper, we use a combination of immunohistochemistry, μCT scanning and histology to analyze the ontogeny of the mandibular and hyoid musculature of the Longnose Gar, *Lepisosteus osseus*. The Longnose Gar, *Lepisosteus osseus*, ranges from Montana to Quebec, south to Florida, and west to northern Mexico. Longnose Gars inhabit slow moving large rivers and lakes and are able to live in poorly oxygenated waters due to their ability to inhale atmospheric oxygen. In Virginia, spawning migration and aggregation to preferred localities upriver occur from mid-May to mid-June (McGrath et al., 2012). This is the first paper of a planned series that will examine the ontogeny of the mandibular and hyoid musculature of basal actinopterygian fishes to facilitate the homologization of individual muscle portions based on their developmental origin.

MATERIALS AND METHODS

Specimens.—All specimens (eggs, larvae, juveniles; see Material Examined) were collected from the Mattaponi River in Virginia and preserved in 4% buffered paraformaldehyde at 4°C overnight and then transferred to 70% ethanol for long-term storage. Specimens were examined and photographed using a Zeiss Discovery V20 (Fig. 1). Some specimens at selected stages were cleared and stained following Taylor and Van Dyke (1985). Lengths were recorded as either notochordal length (NL) or standard length (SL). Specimens of similar developmental stage, which is often, but not always, coherent with size, are described together in the Results. The abbreviations in the subsections of the Results indicate the method that is used (CT = computed tomography, ABS = antibody staining, HIST = histology).

Specimen preparation and imaging.—For the micro-computed tomographic scans (μCT), specimens were treated with phosphotungstic acid following the procedure developed by Metscher (2009a). Specimens were scanned with a X-radia XCT scanner. Based on CT-image stacks of the gar heads, 3D-reconstructions were made using Amira 5.2 (Visage Imaging, Berlin, Germany).

Immunolabeling of the musculature followed a standard protocol for the DAKO EnVision Flex system (Agilent Technologies, Hamburg, Germany). Skeletal muscle tissue was labeled with the monoclonal 12/101 primary antibody (Developmental Studies Hybridoma Bank, University of Iowa, Dept. of Biological Science, Iowa City, IA) and an ALEXA 568 secondary antibody (Invitrogen, Thermo Fisher Scientific Inc., Darmstadt, Germany). Images were taken with a ZEISS LSM 510 controlled by the ZEISS software Zen 2009 and 2012. For histology, a NL 21.5 mm gar was embedded in paraffin and sectioned in 8 μm transverse sections with a HM360 Microm (Germany). The sections were stained using the Heidenhain-Azan technique.

RESULTS

9.2 mm NL (CT); 6.0 mm NL (ABS); Figure 2.—The larvae are comparable to the stage shown in Figure 1E. The yolk sac in the two specimens is a large oval mass. The oral adhesive disc has differentiated and appears to be functional in live specimens. Larvae in this size range are generally passive but start to swim in circles when disturbed. At this stage, skeletal elements could be traced in neither the cleared-and-stained material nor the CT scans. Two small, weakly stained structures are present ventral to the eye (Fig. 2B). Although we could not trace muscle fibers in these as we could in more advanced stages, we interpret the smaller anterior portion as the mandibular muscle and the larger portion as the hyoid muscle primordium. The mandibular muscle primordium is triangular in shape and located just ventral to the eye and dorsoanterior to the dorsal extension of the hyoid muscle primordium. The hyoid muscle primordium (Fig. 2A) is posteroventral to the eye and the mandibular muscle primordium. The hyoid muscle primordium is slightly curved and extends from the dorsoposterior corner of the eye to the ventral midline, and posterior to the mouth (Fig. 2A). The most ventral section extends posteriorly and reaches almost the anterior tip of the yolk sac. Although it is still a single entity, the hyoid muscle primordium has already started to separate, with the ventralmost portion resembling the *m. constrictor hyoideus ventralis* of later stages.

10.0 mm NL (CT); 8.3 and 9.5 mm NL (ABS); Figure 3.—The larvae are comparable to the stage shown in Figure 1F. The yolk sac in larvae of this stage is more elongate and smaller in its diameter than in the previous stage. The larvae still lie on the substrate (e.g., bottom or leaves) and only react to disruptions. At this size range the palatoquadrate consists of the *pars quadrata* and the *pars metapterygoidea* (Fig. 3A). The *processus pterygoideus* has begun to develop. On the posterodorsal margin, the *pars metapterygoidea* has a small posteriorly oriented process. The *pars quadrata*, which forms the ventral part of the palatoquadrate, articulates with Meckel's cartilage. Laterally the palatoquadrate is concave and houses the *m. adductor mandibulae* (Fig. 3B). Meckel's cartilage is a stout element with a medially curved anterior tip (Fig. 3A). The two rami of Meckel's cartilage do not meet each other at this stage. The posterior third of the element is wide, but it tapers again posterior to its articulation with the palatoquadrate. A small socket on the dorsoposterior surface of Meckel's cartilage marks the articulation with the *pars quadrata* (Fig. 3A).

The mandibular muscle primordium is enlarged and divided into three subdivisions, the *m. intermandibularis*, the *m. adductor mandibulae*, and the *m. constrictor mandibularis dorsalis* (Fig. 3B). The most dorsal derivative of the mandibular muscle primordium, the *m. constrictor mandibularis dorsalis*, extends from the anterior part of the otic capsule to the lateral surface of the hyosymplectic cartilage. An extension of the *m. constrictor mandibularis dorsalis* reaches the small process on the dorsoposterior end of the *pars metapterygoidea* (Fig. 3B). The *m. adductor mandibulae* is located ventral to the eye and occupies the lateral groove of the palatoquadrate (Fig. 3B, D, F). The muscle has a pointed posterior end, is wide in its middle section, and bifurcates anteriorly into a broad dorsal and a slender ventral extension. The ventral extension is attached to Meckel's cartilage near its wide anterior edge (Fig. 3B). The most ventral muscle, the *m. intermandibularis*, is attached to the medial sides of Meckel's cartilages (Fig. 3B, C, E, G). In the μCT-scanned specimen this muscle meets its antimere in the midline (Fig. 3C), while in the stained specimens the muscle appears U-shaped, with its open part pointing anteriorly (Fig. 3E, F). The *m. intermandibularis* attaches to the anteriormost tip of the two Meckel's cartilages and is separated from those just posterior to the jaw joint. This muscle becomes smaller in its lateral extension and ends abruptly in the connective tissue of the *m. constrictor hyoideus ventralis*.

Three skeletal elements of the hyoid arch are present at this stage. The most dorsal element is the hyosymplectic cartilage, which articulates with the otic capsule of the neurocranium (Fig. 3A). It is pierced by the foramen for a branch of the facialis nerve (VII). At the anterior tip of the hyosymplectic cartilage, a small anteroventrally oriented process marks the beginning of the symplectic process. The process is not long enough to meet the palatoquadrate. The interhyal cartilage is a small cartilaginous element that connects the hyosymplectic cartilage with the ceratohyal cartilage (we identify this element as the ceratohyal cartilage because the hypohyal cartilage separates from the ceratohyal cartilage in a later stage [see below] and the anterior and posterior ceratohyal will ossify in this portion of the element). The ceratohyal cartilage is obliquely oriented, with its anterior tip located medially and its posterior tip laterally. Posteriorly, the ceratohyal cartilage articulates with the interhyal cartilage (not shown in the 3D-reconstruction in Fig. 3A). Anteriorly the hypohyal cartilage is not yet separated from the ceratohyal cartilage.

The hyoid muscle primordium is divided into two portions (Fig. 3B, D, F). The smaller of the two portions, the *m. constrictor hyoideus dorsalis,* is attached to the medial side of the hyosymplectic cartilage. Both the *m. constrictor hyoideus dorsalis* and the *m. constrictor mandibularis dorsalis* are attached to the otic capsule, the former at a more medial and ventral position than the latter. The *m. constrictor hyoideus ventralis* is the largest muscle at this size. Anteriorly, the *m. constrictor hyoideus ventralis* overlaps the posterior part of the *m. intermandibularis* dorsally. It is attached to the ceratohyal cartilages but extends past them both anteriorly and posteriorly (Fig. 3B, C).

12.8 mm NL (CT); 10.9 mm NL (ABS); Figure 4.—The larvae are comparable to the stages shown in Figure 1F and G. The larvae are similar in their external appearance compared to the previous stage. They also do still not actively swim but do attach to leaves using their adhesive organ. At this size, the most notable difference of the palatoquadrate compared to the previous stage is the initial development of an anterodorsal *processus pterygoideus* (Fig. 4A). The *pars metapterygoidea* extends farther posteriorly and overlaps the symplectic process of the hyosymplectic cartilage. Meckel's cartilage is more elongated than in the previous stage. In addition to the overall elongation of Meckel's cartilage, the left and right rami anterior to the *m. intermandibularis* are recurved and continuous across the midline (Fig. 4C).

The *m. constrictor mandibularis dorsalis* has not changed significantly compared to the previous stage. The most prominent difference is that the anterior extension of the muscle has established a solid connection with the *pars metapterygoidea* (Fig. 4B). The *m. adductor mandibulae* has followed the overall elongation of the palatoquadrate. The tapered posterior end of the muscle is attached to the *pars metapterygoidea* just ventral to the anterior tip of the *m. constrictor mandibularis dorsalis* (Fig. 4B, D). The widened anterior portion of the *m. adductor mandibulae* spans the jaw joint and is attached to Meckel's cartilage with a longer base (Fig. 4B). The dorsally oriented portion, which corresponds to the *m. preorbitalis*, is enlarged as well and reaches the anteroventral margin of the eye.

The hyosymplectic cartilage now has a distinct symplectic process at its anteroventral border that is located ventral to the *pars metapterygoidea* (Fig. 4A). The posterior end of the hyosymplectic cartilage has also differentiated to form the opercular process (Fig. 4A). The anterior end of the ceratohyal cartilage forms a hook-shaped structure that represents the initial development of the hypohyal cartilage (Fig. 4A, B).

The *m. constrictor hyoideus dorsalis* is still an ill-defined muscle on the medial side of the hyosymplectic cartilage. The muscle stretches from the hyosymplectic cartilage posterodorsal to the otic capsule (Fig. 4B). In general the muscle has not changed much in its overall shape compared to the previous stage. In contrast to the dorsal musculature, the *m. constrictor hyoideus ventralis* has changed drastically and is now greatly expanded and more well defined (Fig. 4B, C). The anterior part of this ventral muscle, which is attached to the ceratohyal cartilage, shows an initial separation into the anterior *m. interhyoideus* and the posterior *m. hyohyoideus* (Fig. 4B, C, E).

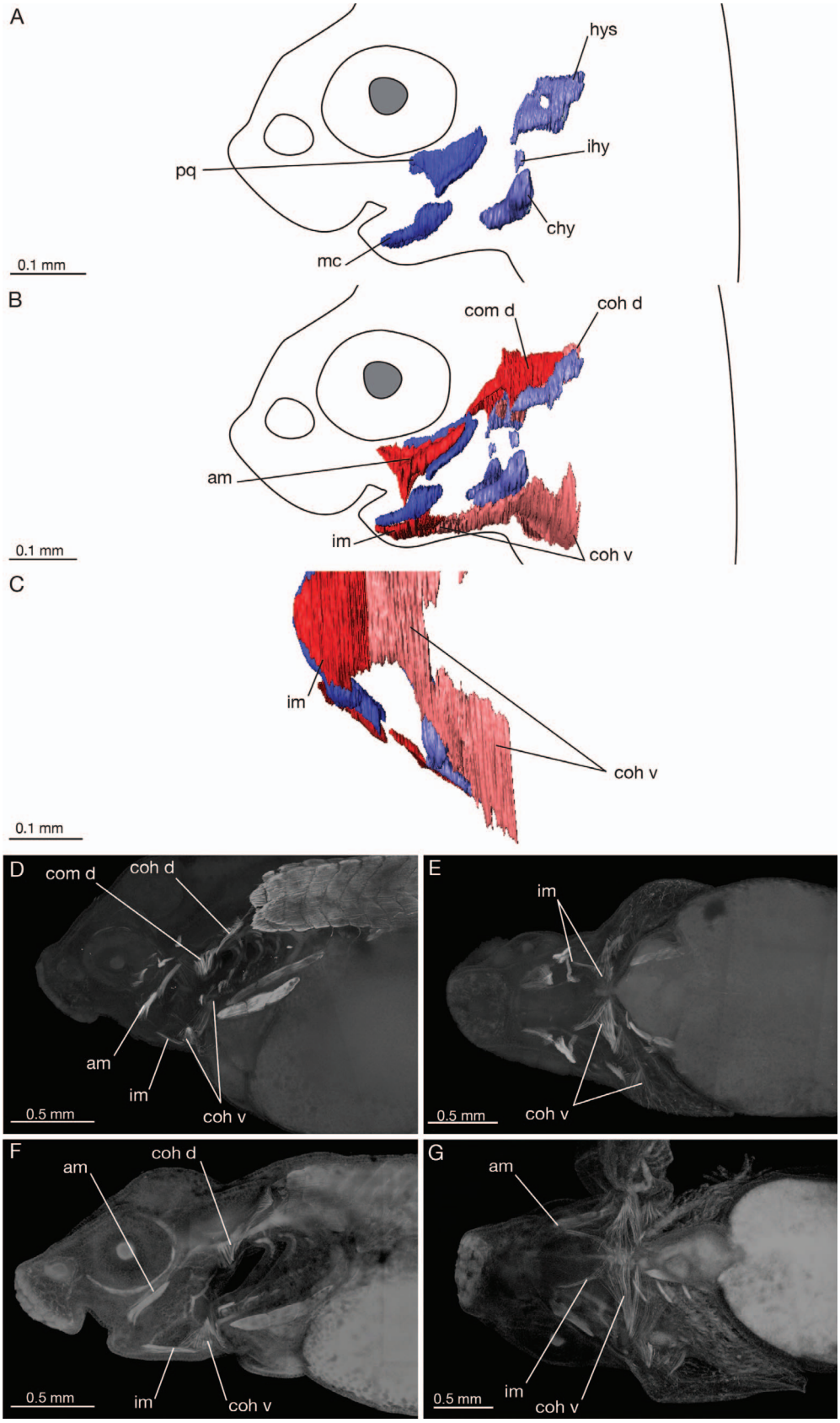

Fig. 3. Reconstructions of a μCT scan of a 10.0 mm NL *Lepisosteus osseus*. (A) Lateral view of a reconstruction of the skeletal elements and (B) of the musculature of the mandibular and hyoid arch. (C) Ventral view of the right side of the ventral portions of the musculature. (D) Lateral and (E) ventral views of confocal images of an 8.3 mm NL and (F) lateral and (G) ventral view of confocal images of a 9.5 mm NL *Lepisosteus osseus*. Abbreviations: am, *musculus adductor mandibulae*; coh d, *musculus constrictor hyoideus dorsalis*; coh v, *musculus constrictor hyoideus ventralis*; chy, ceratohyal cartilage; com d, *musculus constrictor dorsalis*; hys, hyosymplectic cartilage; ihy, interhyal cartilage; im, *musculus intermandibularis*; mc, Meckel's cartilage; pq, palatoquadrate.

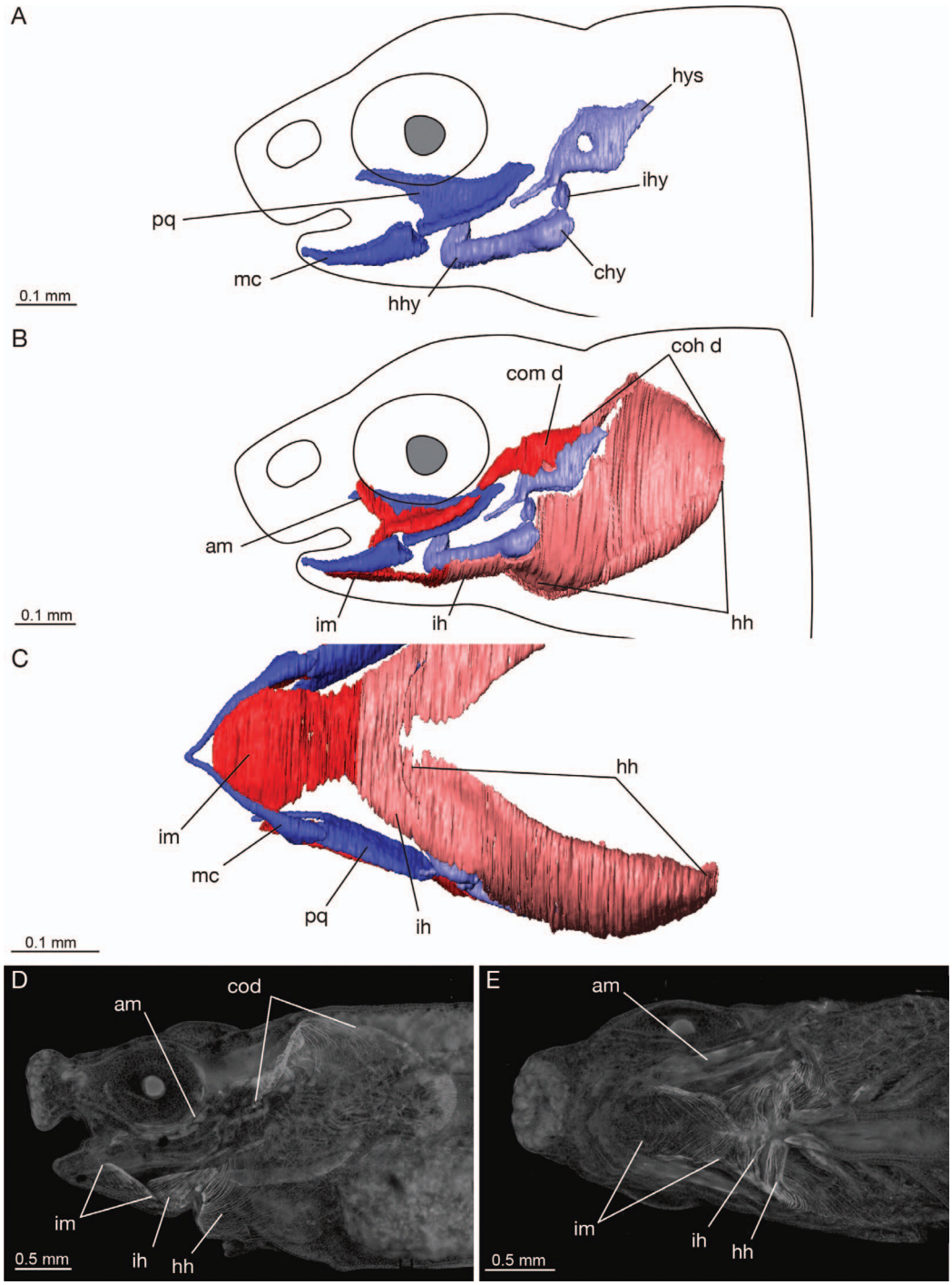

Fig. 4. Lateral and ventral views of reconstructions of a μCT scan of a NL 12.8 mm *Lepisosteus osseus*. (A) Lateral view of the skeletal elements and (B) lateral view of the musculature of the mandibular and hyoid arch. (C) Ventral view of the right side of the ventral portions of the musculature. (D) Lateral and (E) ventral views of confocal images of a 10.9 mm NL *Lepisosteus osseus*. Abbreviations: am, *musculus adductor mandibulae*; chy, ceratohyal cartilage; coh d, *musculus constrictor hyoideus dorsalis*; com d, *musculus constrictor dorsalis*; hh, *musculus hyohyoideus*; hhy, hypohyal cartilage; hys, hyosymplectic cartilage; ih, *musculus interhyoideus*; ihy, interhyal cartilage; im, *musculus intermandibularis*; mc, Meckel's cartilage; pq, palatoquadrate.

16.1 mm SL (CT); 16.1 mm SL (ABS); Figure 5.—The larvae are comparable to the stage shown in Figure 1J. The yolk sac is absorbed and the adhesive disc is reduced at this stage. The larvae are standing upright under the water surface and feed on small zooplankton and other larval fishes. The different regions of the palatoquadrate are more defined compared to previous stages. The *processus pterygoideus* is elongate and follows the growth of the snout (Fig. 5A). Its anterior tip, the *pars autopalatina*, is pointed. The *pars quadrata* has shifted its position anteriorly and the jaw joint is now located below the anterior margin of the eye (Fig. 5A). The *pars metapterygoidea* contacts the hyosymplectic cartilage. In addition to the mandibular ramus, Meckel's cartilage has two additional rami: an anterodorsally oriented coronoid process that almost reaches the *processus pterygoideus*, and a retroarticular process that extends from its posteroventral margin (Fig. 5A). The left and right Meckel's cartilages are continuous anteriorly.

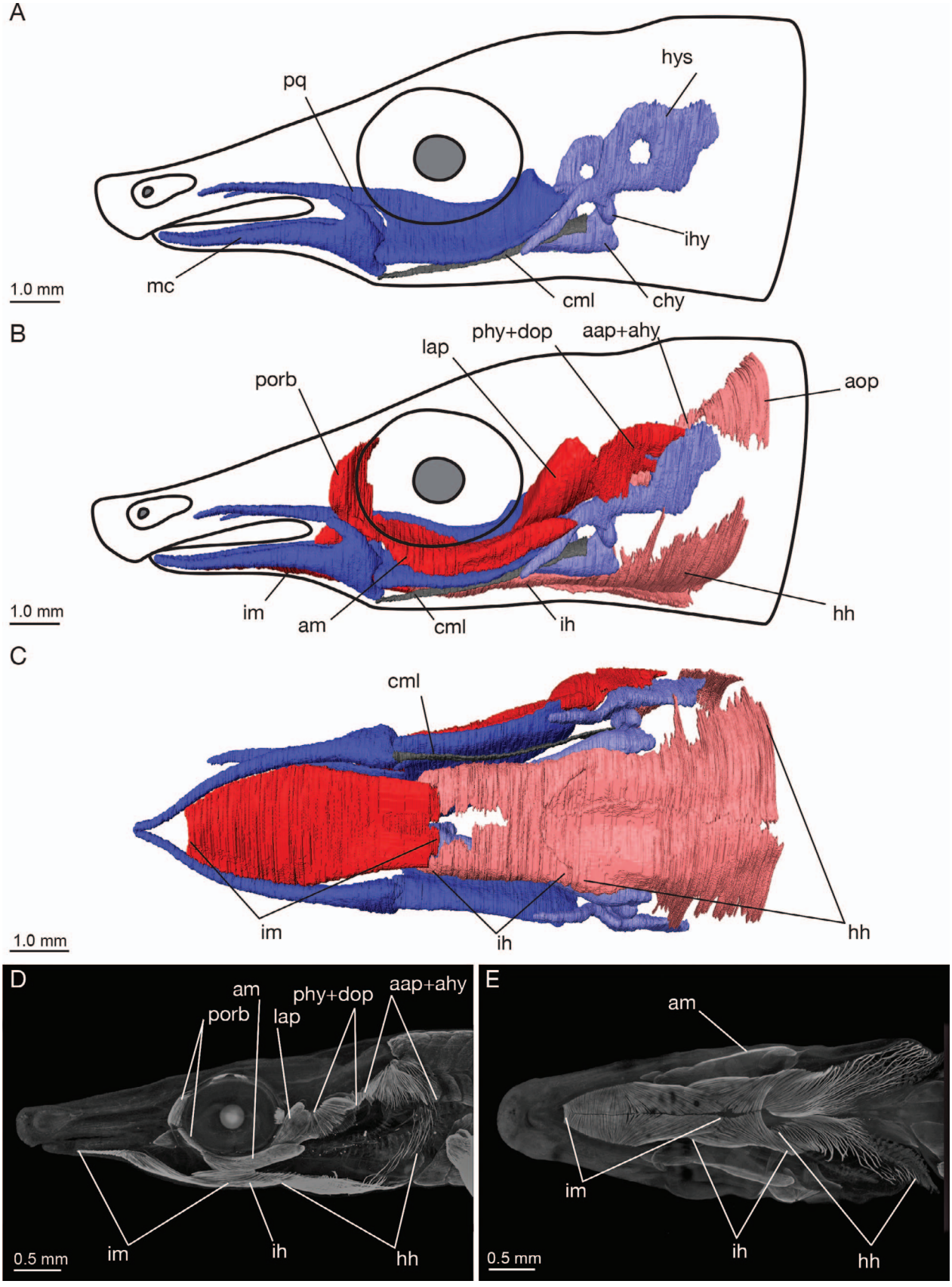

Fig. 5. Lateral and ventral views of reconstructions of a μCT scan of a 16.1 mm SL *Lepisosteus osseus*. (A) Lateral view of the skeletal elements and (B) lateral view of the musculature of the mandibular and hyoid arch. (C) Ventral view of the right side of the ventral portions of the musculature. (D) Lateral and (E) ventral views of confocal images of a 16.1 mm SL *Lepisosteus osseus*. Abbreviations: aap, *musculus adductor arcus palatini*; ahy, *musculus adductor hyomandibulae*; am, *musculus adductor mandibulae*; aop, *musculus adductor operculi*; chy, ceratohyal cartilage; cml, ceratomandibular ligament; dop, *musculus dilatator operculi*; hh, *musculus hyohyoideus*; hys, hyosymplectic cartilage; ih, *musculus interhyoideus*; ihy, interhyal cartilage; im, *musculus intermandibularis*; lap; *musculus levator adductor palatini*; mc, Meckel's cartilage; phy, *musculus protractor hyomandibulae*; porb, *musculus preorbitalis*; pq, palatoquadrate.

The *m. constrictor mandibularis dorsalis* is divided into two partitions at this stage. The anterior partition forms the *m. levator arcus palatini*, which originates on the anterior edge of the otic capsule where the autosphenotic will ossify in later stages (Fig. 5B, E). The muscle inserts on the *pars metapterygoidea* medial to the posterior part of the *m. adductor mandibulae*. The musculature posterior to the *m. levator arcus palatini* represents the *m. protractor hyomandibulae* and the *m. dilatator operculi* (Fig. 5B, E). At this stage the muscle attaches to the lateral surface of the hyosymplectic cartilage and extends down to the foramen hyomandibularis. The *m. adductor mandibulae* is greatly enlarged and its origin is expanded onto the posterior portion of the hyosymplectic cartilage (Fig. 5B, E). Anteriorly the muscle inserts on the medial side of Meckel's cartilage anterior to the coronoid process. The anterodorsal extension of the *m. adductor mandibulae* is much larger as well and is almost separated to become the *m. preorbitalis superficialis* and *profundus* (Fig. 5B, D). The *m. preorbitalis* extends from the insertion point on the proximal end of the coronoid process, up the *lamina orbitonasalis*, until it reaches the roof of the chondrocranium anterior to the eye. Between the proximal part of the *m. preorbitalis* and the *pars quadrata,* a thin muscle bundle has separated from the *m. adductor mandibulae* to form the *m. palatomandibularis* (not shown in figure). It also inserts on the posterior end of Meckel's cartilage. The *m. intermandibularis* attaches to the middle portion of Meckel's cartilage and ends abruptly anterior to the split of the *m. interhyoideus* (Fig. 5C, E).

The anteroventral *pars symplectica* of the hyosymplectic cartilage is more pronounced in this stage than earlier ones and is in contact with the palatoquadrate (Fig. 5A). The posterodorsal head of the hyosymplectic cartilage has widened. The interhyal cartilage is now in contact with both the hyosymplectic cartilage and the ceratohyal cartilage. The ceratohyal cartilage has shifted its position, and its anterior half is located medial to the palatoquadrate (Fig. 5 A). At its anterior tip, the ceratohyal cartilage is separated from the hypohyal cartilage.

The *m. constrictor hyoideus dorsalis* shows signs of partitioning. The thin anterior part, which will presumably give rise to the *m. adductor arcus palatini* and *m. adductor hyomandibulae*, inserts on the hyosymplectic cartilage, while the posterior muscle fibers fade into the opercular flap (Fig. 5B, D). The *m. constrictor hyoideus ventralis* is now completely subdivided into the *m. hyohyoideus* posteriorly and the *m. interhyoideus* anteriorly. The *m. interhyoideus* is attached to the ceratohyal cartilages and merges into the *m. hyohyoideus* posteriorly. The anterior fibers of the *m. hyohyoideus* are attached to the ceratohyal anteriorly and extend into the opercular flap posteriorly to meet the posteriormost muscle fibers of the *m. constrictor hyoideus dorsalis*, representing the precursor of the *m. adductor arcus palatini*, *m. adductor hyomandibulae*, and *m. adductor operculi* (Fig. 5D).

At this stage, we were able to identify the ceratomandibular ligament described by Wiley (1976). As the name of the ligament suggests, it connects the ceratohyal cartilage with Meckel's cartilage (Fig. 5A–C; see also Fig. 6A inset). The anterior attachment of the ligament is on the posterodorsal surface of the ceratohyal cartilage anterior to the interhyal cartilage, and its posterior attachment is on the retroarticular process of Meckel's cartilage.

22.0 mm SL (CT); 21.5 mm SL (HIST); Figures 6 and 7.—The larvae are comparable to the stages shown in Figure 1K and L. The juveniles at this developmental stage swim actively and externally resemble adult gars. The *processus pterygoideus* has stopped following the elongation of the ethmoid region and is in a relatively more posterior position when compared to the previous stage described above (Fig. 6A). The posterior end of the *pars metapterygoidea* now provides a wide surface for attachment of the *m. levator arcus palatini* (Fig. 6A, B, D). The *pars quadrata* and the jaw joint have shifted their positions, and the jaw joint is now located anterior to the eye (Fig. 6A). The left and right Meckel's cartilages are still fused together at the recurved anterior tip (Fig. 6E). The coronoid process has become larger and its distal tip is widened.

The *m. adductor mandibulae* is larger but otherwise appears similar to the condition in the previous stage (Fig. 6B, C). The *m. preorbitalis superficialis* has increased in size as well and surrounds the anterior half of the eyeball (Figs. 6B–D, F, 7D). The smaller *m. preorbitalis profundus* is now present as well and is represented by a small, squarish portion medial to the eye (Figs. 6B–D, F). The two preorbitalis muscles embrace the *m. obliquus superior* eye muscle. The *m. levator arcus palatini* has become larger, and the *m. protractor hyomandibulae* and the *m. dilatator operculi* are still united as one large muscle (Fig. 6B).

The *pars symplectica* of the hyosymplectic cartilage is elongated and reaches the ventral rim of the *pars quadrata*. The anterior part of the ceratohyal cartilage is separated to form the hypohyal cartilage and serves as the insertion point for the *m. sternohyoideus* (Fig. 6A inset). The hypohyal cartilage has a posterodorsally oriented process.

At this stage, the *m. constrictor hyoideus dorsalis* is divided in two partitions (Fig. 6F). The anterior portion represents the *m. adductor arcus palatini* and the *m. adductor hyomandibulae*, attaches to the medial side of the hyosymplectic cartilage, and partially covers the foramen for the *ramus hyomandibularis*. The posterior part, the *m. adductor operculi*, is similar to the situation in the previous stage. The ventral hyoid muscles resemble the situation of the previous stage (Figs. 6E, F, 7A–C).

DISCUSSION

Only a few descriptions of the cranial musculature of adult lepisosteids are available. Luther (1913) described the mandibular and hyoid musculature in *Lepisosteus osseus*; Lauder (1980a) described these in *L. oculatus*. Bodemer (1957) described the development of the extrinsic eye musculature in *L. osseus*. Wiley (1976) described briefly the mandibular and hyoid musculature in lepisosteids generally. Edgeworth's (1911, 1929, 1935) works on the cranial musculature of vertebrates are the only publication that provides ontogenetic data on a wide range of lower actinopterygians, including lepisosteids.

Mandibulohyoid ligament.—Wiley (1976) described a ceratomandibular ligament in gars that connects the posterior ceratohyal to the retroarticular process of the lower jaw (Figs. 5, 6A inset). He hypothesized that this ligament is the functional equivalent of the *m. protractor hyoideus* (herein *m. interhyoideus*; see Winterbottom, 1974) of halecomorph and teleostean fishes, a muscle that Wiley interpreted as only weakly developed in gars. However, the *m. interhyoideus* is a fully developed and large muscle in our specimens (Figs. 4C,

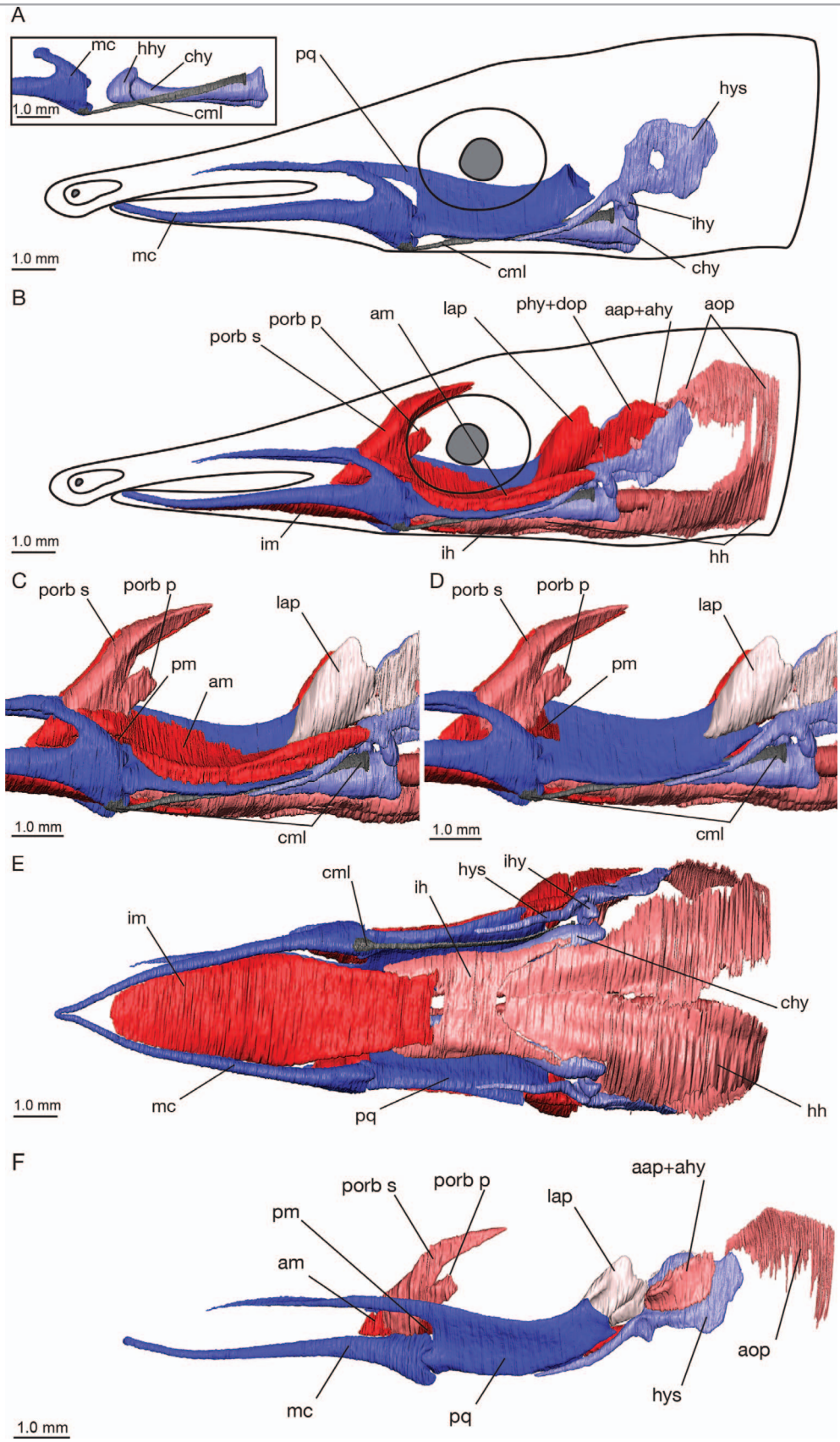

Fig. 6. Lateral and ventral views of reconstructions of a μCT scan of a 22.0 mm SL *Lepisosteus osseus*. (A) Lateral view of the skeletal elements with a close up of the cml and (B) lateral view of the musculature of the mandibular and hyoid arch. (C and D) Lateral views of the musculature (superficial muscles removed in C). (E) Ventral view of the ventral portions of the musculature. (F) Similar view as in D, but with the hyosymplectic cartilage removed. Abbreviations: aap, *musculus arcus palatini*; ahy, *musculus adductor hyomandibulae*; am, *musculus adductor mandibulae*; aop, *musculus adductor operculi*; chy, ceratohyal cartilage; cml, ceratomandibular ligament; dop, *musculus dilator operculi*; hh, *musculus hyohyoideus*; hhy, hypohyal cartilage; hys, hyosymplectic cartilage; ih, *musculus interhyoideus*; ihy, interhyal cartilage; im, *musculus intermandibularis*; lap, *musculus levator adductor palatini*; mc, Meckel's cartilage; phy, *musculus protractor hyomandibulae*; pm, *musculus palatomandibularis*; porb p, *musculus preorbitalis profundus*; porb s, *musculus preorbitalis superficialis*; pq, palatoquadrate.

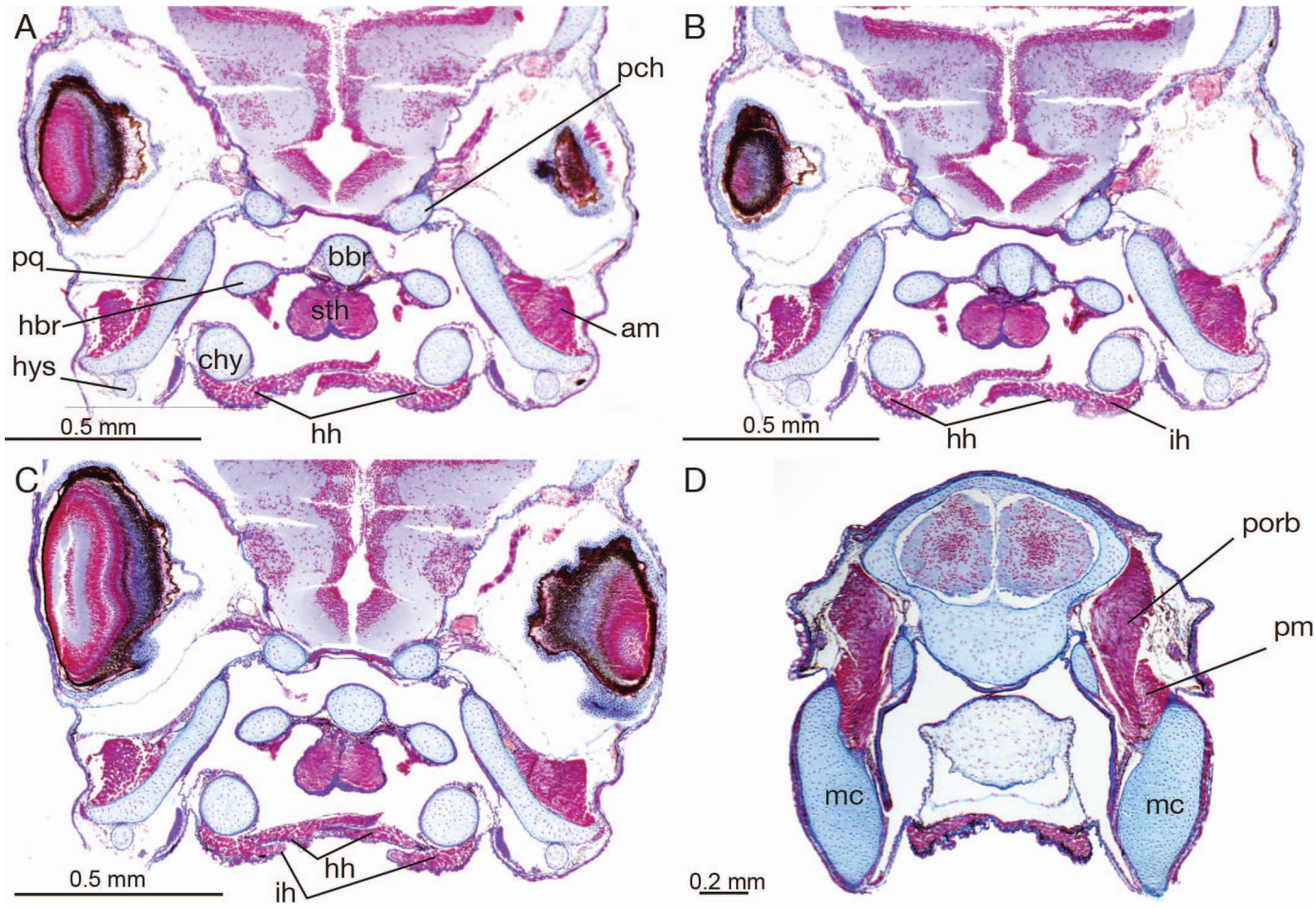

Fig. 7. Histological sections of 21.5 mm SL *Lepisosteus osseus*. (A, B, C) Sections from a mid-region of the head. (D) Section from a more anterior region. Abbreviations: am, *musculus adductor mandibulae*; bbr, basibranchial cartilage; chy, ceratohyal cartilage; hbr, hypobranchial cartilage; hh, *musculus hyohyoideus*; hys, hyosymplectic cartilage; ih, *musculus interhyoideus*; mc, Meckel's cartilage; pch, parachordal cartilage; pm, *musculus palatomandibularis*; porb p, *musculus preorbitalis profundus*; pq, palatoquadrate; sth, sternohyoideus.

5C, 6E, 7B, C). Further, Lauder (1980a) demonstrated that the muscle is active in the expansive phase during the feeding cycle, as in *Amia*, and therefore appears to be fully functional.

In *Amia* the mandibulohyoid ligament originates on the posterior ceratohyal and attaches to the retroarticular (e.g., Allis, 1897; Lauder, 1982) as does the ceratomandibular ligament in lepisosteids; we consider the ligaments to be homologs. The ligament likely serves as the basal mechanical pathway for mandibular depression via the hypaxial musculature, the pectoral girdle, the *m. sternohyoideus*, and the ventral elements of the hyoid arch, that is present in basal actinopterygian and teleostean fishes (Lauder, 1982). Further, Lauder (1982) and Lauder and Liem (1983) hypothesized that the mandibulohyoid ligament of *Amia* and basal teleostean fishes is homologous to the interopercuohyoid ligament of more derived teleostean fishes (Eurypterygia of Wiley and Johnson, 2010) and that its insertion point shifted from the lower jaw to the interopercle during the course of the evolution of actinopterygian feeding mechanisms.

Timing of partitioning of the cranial musculature.—The cranial musculature appears to follow a developmental sequence from single to more complex structures. Both the mandibular and the hyoid primordia begin ontogeny as single entities, and, during the course of development, they divide to become the complex musculature that can be seen in the adult condition. The increasing complexity of the cranial musculature is correlated with the increasing complexity of the supporting skeletal jaw elements and especially with the elongation of the jaws and the ethmoid region. The muscles of the ventral part of the mandibular primordium (*m. intermandibularis* and *m. adductor mandibulae*) differentiate sooner than the muscles of the hyoid primordium (*m. interhyoideus* and *m. hyohyoideus*). Even considering shortcomings of Haeckel's biogenetic law (Haeckel, 1866) and von Baer's four laws of embryology (von Baer, 1828) that are well known (Johnson and Britz, 2005; Konstantinidis and Johnson, 2012), the cranial musculature of *L. osseus* exemplifies the value of ontogenetic data for phylogenetic studies.

Phylogenetic context of ontogeny of the m. adductor mandibulae.—The adductor mandibulae complex of juvenile and adult lepisosteids consists of a main portion, the *m. adductor mandibulae*, and its derivatives, which include the *m. preorbitalis superficialis et profundus* and the *m. palatomandibularis major et minor* (Figs. 5B, E, F, 6B–D, F; subdivisions of the *m. palatomandibularis* are not shown). This complex develops as a single entity after its initial separation from the *m. intermandibularis* and the m. *constrictor dorsalis mandibularis*. Although the complexity of the *m. adductor mandibulae* differs greatly among actinopterygians, a single initial

portion is shown for many other taxa for which ontogeny is known, such as *Amia* (Jarvik, 1980), *Danio rerio* (Hernandez et al., 2005), loricariids (Geerinckx et al., 2007; Huysentruyt et al., 2007), pleuronectiforms (Uji et al., 2010), and tetraodontiforms (Konstantinidis and Harris, 2011). Having a single entity early in development is therefore interpreted to be the plesiomorphic condition for actinopterygian fishes. As a similar condition is found also in chondrichthyans (Edgeworth, 1935) and sarcopterygians (Edgeworth, 1935; Ericsson and Olsson, 2004; Ericsson et al., 2004), it is likely a gnathostome character.

Future of comparative ontogenetic myology.—Over the past 40 years, clearing and double staining has become widely used and has advanced the field of comparative anatomy tremendously. This technique allows examination of fully articulated specimens in large quantities and is relatively inexpensive compared to other approaches to studying early skeletal development (e.g., histological sections and μCT scans). However, a disadvantage of most clearing-and-staining techniques is that soft tissues, such as musculature and nerves, are digested and therefore lost for further analyses. As a consequence, osteological studies, including those with an ontogenetic perspective (although these are still relatively few), greatly outnumber studies of soft tissue. Broadly comparative studies of soft tissue are relatively rare because of difficulties of the lack of sufficient methods and visualization techniques in the past, e.g., antibody staining and computed tomography.

The recent increase in studies of soft tissue development is at least partially related to the adoption of methods (e.g., antibody staining) used in related biological fields, such as developmental biology and genetics. This is concomitant with improved techniques that are in use in morphological studies (e.g., μCT scanning). Antibody staining techniques are a standard method in developmental and molecular biology and have been used for decades, but they are not commonly used in ichthyology and comparative anatomy. Klymkowsky and Hanken (1991) described the technique in *Xenopus,* and Smith (1994) traced the development of the craniofacial musculature in *Monodelphis domestica*. After the initial introduction of the antibody staining method for morphological studies, research groups working on teleostean fishes and tetrapods co-opted the technique for comparative studies (Schilling and Kimmel, 1997; Hernandez et al., 2002, 2005; Ericsson and Olsson, 2004; Olsson et al., 2005; Ziermann and Olsson, 2007; Uji et al., 2010, 2013; Konstantinidis and Harris, 2011).

Micro x-ray computed tomography, or μCT-scanning, has been used for the analysis of skeletal structures in the past, but only very recently has the technique been used to trace the development of soft tissues (Schmidt et al., 2011; Hilton et al., 2015, in this volume). In particular, μCT scans provide three-dimensional data with high resolution that can easily be reconstructed to produce detailed 3D models (for details see Metscher, 2009a, 2009b). These techniques do not replace older ones such as histology and clearing and staining, but rather provide complementary approaches for detailed information (Hilton et al., 2015, in this volume). Further, CT approaches, and to a lesser degree antibody staining, are non-destructive, which makes the techniques attractive for rare specimens. New techniques in morphology such as these have the potential to advance the field of systematic ichthyology and the comparative anatomy of fishes, and we hope that, as the clearing-and-staining method did over four decades ago, they will induce a revolution and motivate ichthyologists to include the development of soft tissue characters in their analyses.

MATERIAL EXAMINED

Institutional abbreviations follow Sabaj Pérez (2014).

Lepisosteus osseus: VIMS 9078 (1 CS); VIMS 12762 (5 CS); VIMS 12968 (6 CS); VIMS 13551 (1 CS); VIMS 13554 (1 CS); VIMS 13559 (developmental series of 285 individuals, including 4 CS and 2 serially sectioned specimens); VIMS 13571 (1 ds); VIMS 13572 (1 ds). Six specimens were scanned for the 3D-reconstructions: VIMS 22683, 9.2 mm NL; VIMS 22684, 10.0 mm NL; VIMS 22685 12.8 mm NL; VIMS 22686, 16.1 mm SL; VIMS 22687, 22.0 mm SL. The six specimens for the immunohistochemistry are combined and listed in one catalogue number, VIMS 22688 (7.1 mm NL, 8.3 mm NL, 9.5 mm NL, 10.9 mm NL, 13.6 mm NL, 16.1 mm SL).

ACKNOWLEDGMENTS

We would like to thank P. McGrath and E. Loose for their help in the field to collect and preserve larval and juvenile gars. We are very grateful to K. Felbel for the histological sections and W. Vogelbein and P. Mason for letting us take advantage of their great microscope setup. We would also like to thank S. Huber for curatorial assistance and G. Arratia and G. D. Johnson for inviting us to contribute to the symposium proceedings. This project was supported by the Volkswagen Foundation, Germany (project no. I84/825 to P. Konstantinidis). This is contribution number 3504 of the Virginia Institute of Marine Science, College of William & Mary.

LITERATURE CITED

Allis, E. P. 1897. The cranial muscles and first spinal nerves in *Amia calva*. Journal of Morphology xii:487–808.

Arratia, G., and H.-P. Schultze. 1991. Palatoquadrate and its ossifications: development and homology within osteichthyans. Journal of Morphology 208:1–81.

Betancur-R, R., R. E. Broughton, E. O. Wiley, K. Carpenter, J. A. López, C. Li, N. I. Holcroft, D. Arcila, M. Sanciangco, J. C. Cureton, II, F. Zhang, T. Buser, M. A. Campbell, J. A. Ballesteros, A. Roa-Varon, S. Willis, W. C. Borden, T. Rowley, P. C. Reneau, D. J. Hough, G. Lu, T. Grande, G. Arratia, and G. Ortí. 2013. The tree of life and a new classification of bony fishes. PLOS Currents Tree of Life. 2013 Apr 18. Edition 1. DOI: 10.1371/currents.tol.53ba26640df0ccaee75bb165c8c26288.

Bodemer, C. W. 1957. The origin and development of the extrinsic ocular muscles in the gar pike (*Lepisosteus osseus*). Journal of Morphology 100:83–111.

Britz, R., and G. D. Johnson. 2010. Occipito-vertebral fusion in actinopterygians: conjecture, myth and reality. Part 1: Non-teleosts, p. 77–93. *In:* Mesozoic Fishes 4—Homology and Phylogeny. J. S. Nelson, H.-P. Schultze, and M. V. H. Wilson (eds.). Verlag Dr. Friedrich Pfeil, München.

Cavin, L. 2010. Diversity of Mesozoic semionotiform fishes and the origin of gars (Lepisosteidae). Naturwissenschaften 97:1035–1040.

Edgeworth, F. H. 1911. On the morphology of the cranial muscles in some vertebrates. Quarterly Journal of Microscopical Science 56:167–316.

Edgeworth, F. H. 1929. II. The development of some of the cranial muscles of ganoid fishes. Philosphical Transactions of the Royal Society London Biological Science 217:39–89.

Edgeworth, F. H. 1935. The Cranial Muscles of Vertebrates. Cambridge University Press, London.

Ericsson, R., R. Cerny, P. Falck, and L. Olsson. 2004. Role of cranial neural crest cells in visceral arch muscle positioning and morphogenesis in the Mexican axolotl, *Ambystoma mexicanum*. Developmental Dynamics 231:237–247.

Ericsson, R., and L. Olsson. 2004. Patterns of spatial and temporal visceral arch muscle development in the Mexican Axolotl (*Ambystoma mexicanum*). Journal of Morphology 261:131–140.

Gardiner, B. G. 1960. A revision of certain actinopterygian and coelacanth fishes, chiefly from the Lower Lias. Bulletin of the British Museum (Natural History), Geology 8:258–325.

Gardiner, B. G., D. T. J. Littlewood, and J. G. Maisey. 1996. Interrelationships of basal neopterygians, p. 117–146. *In:* Interrelationships of Fishes. M. L. J. Stiassny, L. R. Parenti, and G. D. Johnson (eds.). Academic Press, San Diego, California.

Geerinckx, T., M. Brunain, and D. Adriaens. 2007. Development of the osteocranium in the suckermouth armored catfish *Ancistrus* cf. *triradiatus* (Loricariidae, Siluriformes). Journal of Morphology 268:254–274.

Gegenbaur, C. 1887. Ueber die Occipitalregion und die ihr benachbarten Wirbel der Fische. *In:* Festschrift Albert von Kölliker zur Feier seines siebenzigsten Geburtstages gewidmet von seinen Schülern. W. Engelmann, Leipzig.

Goodrich, E. S. 1930. Studies on the Structure and Development of Vertebrates. Macmillan, London.

Grande, L. 2010. An empirical synthetic pattern study of gars (Lepisosteiformes) and closely related species, based mostly on skeletal anatomy. The resurrection of Holostei. American Society of Ichthyologists and Herpetologists, Special Publication 6.

Haeckel, E. H. P. A. 1866. Generelle Morphologie der Organismen. II. Georg Reimer, Berlin.

Hammarberg, F. 1937. Zur Kenntnis der Ontogenetischen Entwicklung des Schädels von *Lepisosteus platystomus*. Acta Zoologica 18:210–336.

Hernandez, L. P., M. J. F. Barresi, and S. H. Devoto. 2002. Functional morphology and developmental biology of zebrafish: reciprocal illumination from an unlikely couple. Integrative and Comparative Biology 42:222–231.

Hernandez, L. P., S. E. Patterson, and S. H. Devoto. 2005. The development of muscle fiber type identity in zebrafish cranial muscles. Anatomy and Embryology 209:323–334.

Hilton, E. J., P. Konstantinidis, N. K. Schnell, and C. B. Dillman. 2014. Identity of a unique cartilage in the buccal cavity of gars (Neopterygii: Lepisosteiformes: Lepisosteidae). Copeia 2014:50–55.

Hilton, E. J., N. K. Schnell, and P. Konstantinidis. 2015. When tradition meets technology: systematic morphology of fishes in the early 21st Century. Copeia 103:858–873.

Huxley, T. H. 1861. Preliminary essay upon the systematic arrangement of the fishes of the Devonian epoch. Memoires of the Geological Survey of the United Kingdom 10:1–40.

Huysentruyt, F., T. Geerinckx, and D. Adriaens. 2007. A descriptive myology of *Corydoras aeneus* (Gill, 1858) (Siluriformes: Callichthyidae), with a brief discussion on adductor mandibulae homologies. Animal Biology 57:433–452.

Inoue, J. G., M. Miya, K. Tsukamoto, and M. Nishida. 2003. Basal actinopterygian relationships: a mitogenomic perspective on the phylogeny of the "ancient fish". Molecular Phylogenetics and Evolution 26:110–120.

Jarvik, E. 1980. Basic structure and evolution of vertebrates, p. i–xvi, 1–575. *In:* Basic Structure and Evolution of Vertebrates. Vol. 1. Academic Press, London, New York.

Jenkins, R. E., and N. M. Burkhead. 1993. Freshwater Fishes of Virginia. American Fisheries Society, Bethesda, Maryland.

Jessen, H. 1972. Schultergürtel und Pectoralflosse bei Actinopterygiern. Fossil Strata 1:1–101.

Johnson, G. D., and R. Britz. 2005. Leis' conundrum: homology of the clavus of the ocean sunfishes. 2. Ontogeny of the median fins and axial skeleton of *Ranzania laevis* (Teleostei, Tetraodontiformes, Molidae). Journal of Morphology 266:11–21.

Kammerer, C. F., L. Grande, and M. W. Westneat. 2006. Comparative and developmental functional morphology of the jaws of living and fossil gars (Actinopterygii: Lepisosteidae). Journal of Morphology 267:1017–1031.

Klymkowsky, M. W., and J. Hanken. 1991. Whole-mount staining of *Xenopus* and other vertebrates, p. 419–441. *In:* Methods in Cell Biology. Vol. 36. B. K. Kay and H. B. Peng (eds.). Academic Press, San Diego.

Konstantinidis, P., and M. P. Harris. 2011. Same but different: ontogeny and evolution of the musculus adductor mandibulae in the Tetraodontiformes. Journal of Experimental Zoology Part B 316:10–20.

Konstantinidis, P., and G. D. Johnson. 2012. A comparative ontogenetic study of the tetraodontiform caudal complex. Acta Zoologica 93:98–114.

Kryzanovsky, S. 1927. Die Entwicklung der paarigen Flossen bei *Acipenser*, *Amia* und *Lepidosteus*. Acta Zoologica 8:278–352.

Lauder, G. V. 1980a. Evolution of the feeding mechanism in primitive actinopterygian fishes—a functional anatomical analysis of *Polypterus*, *Lepisosteus*, and *Amia*. Journal of Morphology 163:283–317.

Lauder, G. V. 1980b. On the evolution of the jaw adductor musculature in primitive gnathostome fishes. Breviora: 1–10.

Lauder, G. V. 1982. Patterns of evolution in the feeding mechanism of actinopterygian fishes. American Zoologist 22:275–285.

Lauder, G. V., and K. F. Liem. 1983. The evolution and interrelationships of the actinopterygian fishes. Bulletin of the Museum of Comparative Zoology 150:95–197.

Lecointre, G., H. Philippe, H. L. Vanle, and H. Leguyader. 1994. How many nucleotides are required to resolve a phylogenetic problem? The use of a new statistical method applicable to available sequences. Molecular Phylogenetics and Evolution 3:292–309.

Long, W. L., and W. W. Ballard. 2001. Normal embryonic stages of the longnose gar, *Lepisosteus osseus*. BMC Developmental Biology 1:6.

Luther, A. 1913. Ueber die vom N. trigeminus versorgte Muskulatur der Ganoiden und Dipneusten. Helsingfors Acta Societas Scientiarum Fennica 41:1–72.

Mayhew, R. L. 1924. The skull of *Lepidosteus platostomus*. Journal of Morphology 38:315–346.

McGrath, P. E., E. J. Hilton, and J. A. Musick. 2012. Seasonal distribution and movements of longnose gar (*Lepisosteus osseus*) within the York River System, Virginia. Southeastern Naturalist 11:375–386.

Metscher, B. D. 2009a. MicroCT for comparative morphology: simple staining methods allow high-contrast 3D imaging of diverse non-mineralized animal tissues. BMC Physiology 9:11.

Metscher, B. D. 2009b. MicroCT for developmental biology: a versatile tool for high-contrast 3D imaging at histological resolutions. Developmental Dynamics 238:632–640.

Normark, B. B., A. R. McCune, and R. G. Harrison. 1991. Phylogenetic relationships of neopterygian fishes, inferred from mitochondrial DNA sequences. Molecular Biology and Evolution 8:819–834.

Olsen, P. E., and A. R. McCune. 1991. Morphology of the *Semionotus elegans* species group from the Early Jurassic part of the Newark supergroup of eastern North America with comments on the family Semionotidae (Neopterygii). Journal of Vertebrate Paleontology 4:481–499.

Olsson, L., R. Ericsson, and R. Cerny. 2005. Vertebrate head development: segmentation, novelties, and homology. Theory in Biosciences 124:145–163.

Patterson, C. 1973. Interrelationships of holosteans, p. 233–305. *In:* Interrelationships of Fishes. P. H. Greenwood, R. S. Miles, and C. Patterson (eds.). Academic Press, London.

Piekarski, N., and L. Olsson. 2007. Muscular derivatives of the cranialmost somites revealed by long-term fate mapping in the Mexican axolotl (*Ambystoma mexicanum*). Evolution & Development 9:566–578.

Romer, A. S. 1966. Vertebrate Paleontology. University of Chicago Press, Chicago.

Rosen, D. E., P. L. Forey, B. G. Gardiner, and C. Patterson. 1981. Lungfishes, tetrapods, paleontology and plesiomorphy. Bulletin of the American Museum of Natural History 167:159–176.

Sabaj Pérez, M. H. (Ed.). 2014. Standard symbolic codes for institutional resource collections in herpetology and ichthyology: an Online Reference. Version 5.0 (22 September 2014). Electronically accessible at http://www.asih.org/, American Society of Ichthyologists and Herpetologists, Washington, D.C.

Schilling, T. F., and C. B. Kimmel. 1997. Musculoskeletal patterning in the pharyngeal segments of the zebrafish embryo. Development 124:2945–2960.

Schmalhausen, J. J. 1913. Zur Morphologie der unpaaren Flossen. II. Bau und Phylogenese der unpaaren Flossen und insbesonders der Schwanzflosse der Fische. Zeitschrift für wissenschaftliche Zoologie 104:1–80.

Schmidt, J., M. Schuff, and L. Olsson. 2011. A role for FoxN3 in the development of cranial cartilages and muscles in *Xenopus laevis* (Amphibia: Anura: Pipidae) with special emphasis on the novel rostral cartilages. Journal of Anatomy 218:226–242.

Sewertzoff, A. N. 1895. Die Entwicklung der Occipitalregion der niederen Vertebraten im Zusammenhang mit der Frage nach der Metamerie des Kopfes. Bulletin de la societe imperiale des naturalistes de Moscou 9:186–284.

Smith, K. K. 1994. Development of craniofacial musculature in *Monodelphis domestica* (Marsupialia, Didelphidae). Journal of Morphology 222:149–173.

Staab, K. L., and L. P. Hernandez. 2010. Development of the cypriniform protrusible jaw complex in *Danio rerio*: constructional insights for evolution. Journal of Morphology 271:814–825.

Taylor, W. R., and C. C. Van Dyke. 1985. Revised procedures for staining and clearing small fishes and other vertebrates for bone and cartilage study. Cybium 9:107–120.

Uji, S., T. Kurokawa, and T. Suzuki. 2010. Muscle development in the japanese flounder, *Paralichthys olivaceus*, with special reference to some of the larval-specific muscles. Journal of Morphology 271:777–792.

Uji, S., T. Seikai, T. Suzuki, and K. Okuzawa. 2013. Muscle development in the bamboo sole *Heteromycteris japonicus* with special reference to larval branchial levators. Journal of Fish Biology 83:1–13.

Veit, O. 1907. Über einige Besonderheiten am Primordialcranium von *Lepidosteus osseus*. Anatomische Hefte 99:155–204.

von Baer, K. E. 1828. Ueber die Entwicklungsgeschichte der Thiere: Beobachtung und Reflexion. Bornträger, Königsberg.

Werneburg, I., and S. T. Hertwig. 2009. Head morphology of the ricefish, *Oryzias latipes* (Teleostei: Beloniformes). Journal of Morphology 270:1095–1106.

Wiley, E. O. 1976. The phylogeny and biogeography of fossil and Recent gars (Actinopterygii: Lepisosteidae). University of Kansas Museum of Natural History Miscellaneous Publications 64:1–111.

Wiley, E. O., and G. D. Johnson. 2010. A teleost classification based on monophyletic groups, p. 123–182. *In:* Mesozoic Fishes 4—Homology and Phylogeny. J. S. Nelson, H.-P. Schultze, and M. V. H. Wilson (eds.). Verlag Dr. Friedrich Pfeil, München.

Winterbottom, R. 1974. A descriptive synonymy of the striated muscles of the Teleostei. Proceedings of the Academy of Natural Sciences of Philadelphia 125:225–317.

Ziermann, J. M., and L. Olsson. 2007. Patterns of spatial and temporal cranial muscle development in the African clawed frog, *Xenopus laevis* (Anura: Pipidae). Journal of Morphology 268:791–804.